PCCP

Accepted Manuscript

ROYAL SOCIETY OF CHEMISTRY

www.rsc.org/pccp

Physical Chemistry Chemical Physics

ARTICLE

Preparation of graphene oxide and polymer-like quantum dots and their one- and two-photon induced fluorescence properties

Received 00th January 20xx,
Accepted 00th January 20xx

DOI: 10.1039/x0xx00000x

www.rsc.org/

Jia Jia Huang,[ab] Min Zhi Rong*[b] and Min Qiu Zhang*[b]

A simple, effective and green bottom-up method for the synthesis of highly fluorescent N doped graphene oxide quantum dots (GOQDs) and polymer-like quantum dots (PQDs) was developed on the basis of rapid one-step microwave assisted pyrolysis of citric acid (CA) and diethylenetriamine (DETA) in different reaction solvents. Both one-photon-induced and two-photon-induced photoluminescence (PL) properties of the resultant GOQDs and PQDs were characterized and analyzed. The one-photon-induced PL quantum yields (QY) of GOQDs and PQDs reached to 39.8 and 74.0%, respectively, which are high enough to exhibit strong photoluminescence (PL) emission even under daylight excitation. The origin of the PL behavior and PL quenching mechanism was explored in terms of the interaction between the functional groups on the surfaces of GOQDs or PQDs and Hg^{2+}. Furthermore, due to the excellent selectivity and sensitivity of the GOQDs and PQDs to Hg^{2+}, the quantum dots might be used for quantitative detection of Hg^{2+} in aqueous solution.

1 Introduction

Fluorescent graphene-based quantum dots (like graphene quantum dots (GQDs), graphene oxide quantum dots GOQDs, etc.) that combine the excellent properties of carbon dots and graphene have attracted substantial research attention recently.[1-3] Top-down method was mostly used to prepare fluorescent graphene-based quantum dots by cutting carbon resources such as graphene, graphene oxide (GO), graphite, carbon fibers and carbon black in terms of hydrothermal, reoxidation, electrochemical or chemical oxidation routes.[4-14] However, some disadvantages exist in the methods, including the requirement of special equipments, low yield, critical synthesis conditions, non-selectivity, etc.[15,16]

Meanwhile, bottom-up method was also developed to fabricate fluorescent graphene-based quantum dots through carbonizing organic precursors by pyrolysis or stepwise solution chemistry, which could provide the products with well-defined molecular size and morphology.[17-20] Nevertheless, the low quantum yield (QY) (used to be less than 10%) limits their applications in practice.

Microwave assisted pyrolysis have been widely used to prepare carbon dots owing to its low-cost, high efficiency, environment friendly and simplicity.[21-24] To the best of our knowledge, there are few reports about the preparation of fluorescent graphene-based quantum dots with this technique.[25,26] In this paper, N doped fluorescent GOQDs and polymer-like quantum dots (PQDs) are synthesized via rapid one-step microwave assisted pyrolysis of citric acid (CA) and diethylenetriamine (DETA) in different reaction solvents. The resultants can be easily purified by repeatedly washing with ethanol. The fabrication is simple, efficient, green and more importantly, QY of the GOQDs and PQDs are high enough to exhibit strong photoluminescence (PL) emission even under daylight excitation. Besides, the GOQDs and PQDs have obvious two-photoninduced PL property. They exhibit outstanding selectivity and sensitivity to Hg^{2+} and hence can be used for quantitative detection of Hg^{2+} in aqueous solution.

2 Experimental

2.1 Reagents and materials

Citric acid (CA, 99.5%) and diethylenetriamine (DETA, 99%)were supplied by Aldrich. Other chemicals (AR) were purchased from Guangzhou Chemical Reagent Factory, China. Ultra-purified water was used throughout all the experiments.

2.2 Synthesis of N doped GOQDs and PQDs

The N doped GOQDs and PQDs were prepared by microwave-assisted pyrolysis (Scheme 1). Typically, CA (1g) was dissolved in the mixture of ultra-purified water (1 ml), glycerol (1g) and DETA (200 μL), which was then heated in a 750 W microwave oven for 5-10 min. With a rise in time, the color of the solution changed from colorless to yellow and black. When the reaction was finished, sheeted GOQDs were obtained. The products were washed with ethanol for several times to remove the

[a] School of Chemical Engineering and Energy, School of Materials Science and Engineering, Zhengzhou University, Zhengzhou 450001, P. R. China
[b] Key Laboratory for Polymeric Composite and Functional Materials of Ministry of Education, GD HPPC Lab, School of Chemistry and Chemical Engineering, Sun Yat-sen University, Guangzhou 510275,P. R. China. Fax: (+86)20 84114008; Tel: (+86)20 84114008;E-mail: cesrmz@mail.sysu.edu.cn, ceszmq@mail.sysu.edu.cn
Electronic Supplementary Information (ESI) available: supporting Tables and Figures.See DOI:10.1039/b000000x/.

residual small molecules, and then dispersed in water. The particles that could not be dispersed were removed through centrifugation. After freeze drying of the aqueous solution for 48h, GOQDs solid (0.88g) was yielded. The PQDs were prepared through the same method in the absence of glycerol.

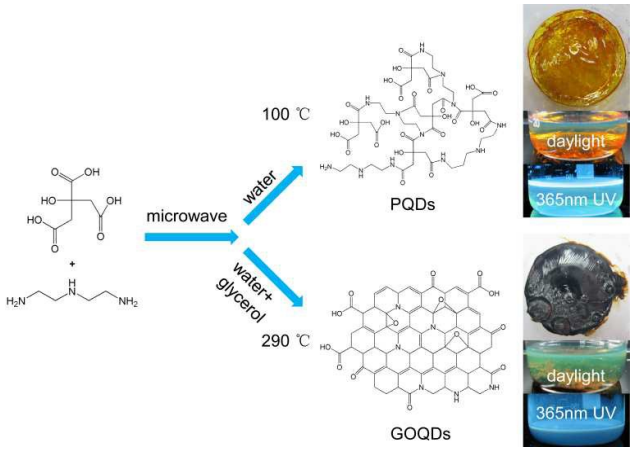

Scheme 1.Schematic illustration of the formation of PQDs and GOQDs.

2.3 Quenching effect of Hg^{2+}

Detection test of Hg^{2+} was performed at room temperature in ultra-purified water. To evaluate the selectivity, various metal ions and oxidant were dissolved in the water with certain concentrations, followed by the addition of calculated amounts of GOQDs and PQDs, respectively. The PL spectra were recorded after 15min. The sensitivity experiments were conducted in the same way. All the measurements were carried out in triplicate.

2.4 Characterization

Transmission electron microscopy (TEM) and high resolution transmission electron microscopy (HRTEM) images were taken by FEI Tecnai G^2 F30. Atomic force microscopy (AFM) images were recorded on Bruker Multimode-8. Ultraviolet-visible (UV-vis) absorption spectra were collected using PE-Lambda 750 UV-vis-NIR spectrophotometer. PL were obtained by a FLS920 combined time resolved & steady state fluorescence spectrometer (Edinburgh Instruments) using the 350 nm line of an Xe lamp as the excitation source and R1527 photomultiplier tube as the detector. For the fluorescence lifetime measurement, a pico-second pulsed diode laser was used to excite the samples. The pulse width, wavelength, and repetition rate were chosen as 100 ps, 405 nm, and 5 MHz, respectively. X-ray photoelectron spectroscopy (XPS) measurements were performed on an ESCALAB-MKII 250 photoelectron spectrometer (VG Co.) with AlK_α X-ray radiation as the X-ray source for excitation. Infrared spectra were collected on a VERTEX Fourier transform infrared (FTIR) spectrometer (Bruker). Thermal gravimetric analysis (TGA) was performed on a TA Q50 analyzer (TA Instruments) under nitrogen atmosphere at a heating rate of 10 °C/min. TGA-FTIR were collected on a STA449F3/Nicolet 6700 thermogravimetry-Fourier transform infrared spectrometry (Netzsch, Germany) under nitrogen atmosphere at a heating rate of 10 °C/min. Nuclear magnetic resonance (NMR) was done on AVANCEIII400 (Bruker). Elemental analysis (EA) was performed on a Vario EL (Elementar) elemental analyzer. Quantum yield measurements were conducted according to ref.[27]. A quinine sulphate in 0.1 M H_2SO_4 solution (with literature quantum yield of 54 % at 360 nm) was used as the standard. The calculation of quantum yield followed the equation: $Y=Y_{st}(I/I_{st})(F_{st}/F)(n/n_{st})^2$, where Y is the quantum yield, I is the integrated area under the emission spectrum, F is the absorbance at the excitation wavelength, and n is the refractive index of the solvent. The subscript "*st*" refers to standard with the known quantum yield. To minimize the reabsorption effect, absorption in the 10 mm fluorescence cuvette was kept below 0.10 at the excitation wavelength.

3 Results and discussion

The GOQDs and PQDs prepared by the one-pot microwave-assisted pyrolysis were formed through inter- and intra-molecular dehydration between CA and DETA and further carbonization.[27]Glycerol that has higher boiling point than water helps to increase the reaction temperature of the system under microwave irradiation. As a result, the GOQDs with higher degree of carbonation were obtained at higher temperature, while the PQDs had to be produced at lower temperature due the absence of glycerol. In addition, because the PQDs and GOQDs can not be dispersed in ethanol while CA and DETA have good solubility in ethanol, the reaction products can be easily purified by ethanol washing.

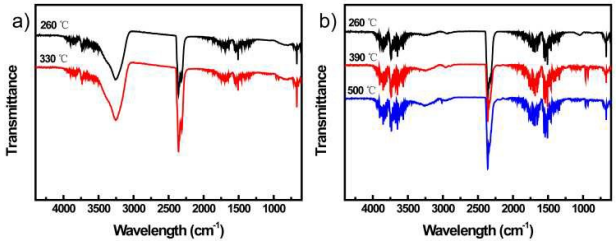

Fig. 1 FTIR spectra of the gases produced by (a) PQDs and (b) GOQDs at different temperatures in N_2.

To understand the formation mechanism of PQDs and GOQDs, thermogravimetric analysis (TGA) coupled with Fourier transform infrared (FTIR) spectroscopy was carried out. As shown in Fig. 1a, when the PQDs are heated to 260 °C, H_2O (3261 cm^{-1}) and CO_2 (2359, 2344, 669 cm^{-1}) along with some amides (3736 cm^{-1} (ν_{NH}), 1684 cm^{-1} ($\nu_{C=O}$), 1508 cm^{-1} (ν_{C-N})) are discharged. In the case of higher temperature of 330 °C, a few NH_3 (964, 929 cm^{-1}) are observed. The appearance of H_2O represents incomplete intermolecular dehydration of CA and DETA, while the other peaks and the element analysis results (Table S1) prove that the PQDs are the condensation product of CA and DETA. With respect to the GOQDs (Fig. 1b), no H_2O is generated during heating. They have higher carbon content and lower nitrogen content than PQDs (Table S1). It means that the GOQDs might be obtained by dehydration, desamidization, decarbonation and deamination of PQDs.

Surface chemistry of GOQDs and PQDs was investigated by XPS and FTIR (Fig. 2). Three types of carbon are found on GOQDs and PQDs: graphitic or aliphatic (C=C and C-C), oxygenated carbon and nitrous carbon (Fig. 2a, b).[27] The percentage of carbon in GOQDs is higher than that in PQDs (Table S2), indicating that the higher degree of carbonation of GOQDs. It agrees with the elemental analysis results of GOQDs and PQDs (Table S1). There are also three types of nitrogen on PQDs and GOQDs: pyridinic C-N-C, pyrrolic C2-N-H, and graphitic N-C3 (Fig. S1).[20,28] On the FTIR spectra of GOQDs (Fig. 2c), the broad peak centered at 3366 cm^{-1} is attributed to stretching vibration of O-H and N-H. Along with the stretching of C=O at 1701 cm^{-1}, it can be concluded that there are extensive carboxyl groups on the surface of GOQDs. Additionally, the peaks at 1655, 1561 and 1402 cm^{-1} are assigned to the amide I and II bands and $\nu_{C\text{-}N}$ of amide linkage (-CONH-), while the peak at 1044 cm^{-1} arises from $\nu_{C\text{-}O\text{-}C}$. The PQDs have similar FTIR characteristics as GOQDs. On the ^{13}C NMR spectrum of GOQDs (Fig. 2d), the signals in the range of 20-80 ppm correspond to aliphatic (sp^3) carbon atoms, while those from 100 to 185 ppm correspond to sp^2 carbon atoms. [27]

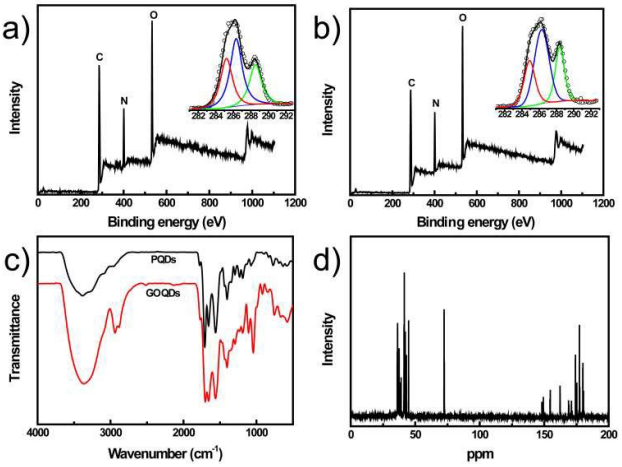

Fig. 2 (a) and (b) XPS spectra of PQDs and GOQDs. (c) FTIR spectra of PQDs and GOQDs. (d) ^{13}C NMR spectrum of GOQDs.

Due to the low degree of condensation, it was hard to get TEM image of PQDs. TEM image of GOQDs is given in Fig. 3a and 3c, which shows that the GOQDs have a uniform dispersion without apparent aggregation and the size of the single GOQDs ranges from 2 to 5 nm. The HTEM image further illustrates that most particles of GOQDs have clear lattice structure. The lattice planes with interplanar spacing of 0.206 nm are close to (102) facets of sp^2 graphitic carbon,[29] implying that the GOQDs are structured like crystalline graphite carbon. Due to the interference of fluorescence, however, no obvious D or G band was detected in the Raman spectra of GOQDs. The topographic morphology of GOQDs measured by AFM reveals that the height of GOQDs ranges between 0.5 and 3.5 nm (Fig. 3b and 3d), corresponding to 1~5 graphene oxide layers. Moreover, most single particle has a platform structure, a main feature of graphene (Fig. S2).

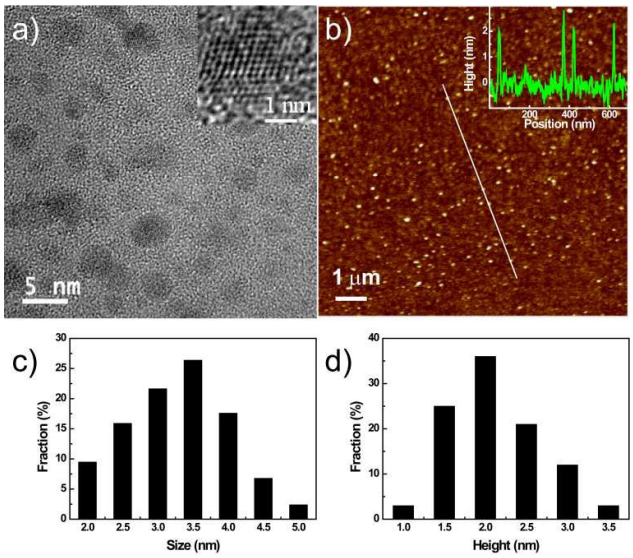

Fig. 3 (a) TEM image of GOQDs (inset: HRTEM image of single GOQDs). (b) AFM topography image of GOQDs (inset: height profile along the white line on the topography image). (c) Size distribution of GOQDs determined by TEM. (d) height distribution of GOQDs determined by AFM.

The XRD profile of the GOQDs shows a broad (002) peak centered at ~20° (Fig. 4a), which is similar to the GOQDs synthesized by other methods.[25,30] However, there is no obvious peak in the XRD pattern of the PQDs. In the UV/Vis spectra (Fig. 4b), the absorption peaks at 240nm and 350nm are assigned to π-π* (K band) and n-π* (R band) of conjugated C=C, which is quite similar to the reported GOQDs.[15]

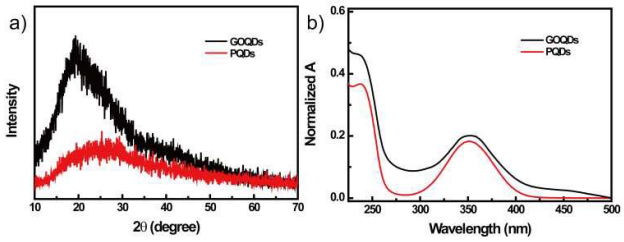

Fig. 4 (a) UV-vis absorption spectra and (b) XRD patterns of GOQDs and PQDs.

Photoluminescence (PL) tests found that both PQDs and GOQDs have excellent fluorescence property. Their QYs are 74.0 and 39.8% (using quinine sulfate as the reference), respectively (Fig. S3), which are higher than the QYs of most carbon-based dots.[15,27,31] The strong fluorescence can even be observed under daylight excitation (Fig. S4). As shown in the PL spectra of PQDs and GOQDs (Fig. 5a and 5b), there are two obvious excitation peaks at 250 and 355 nm, well agreeing with the absorption peaks on the UV/Vis spectra. However, the emission peaks excited at 250 or 355 nm have no shift, and the emission intensity is dependent on excitation intensity. This means that there are at least two types of excitation centers and only one type of emission center in PQDs or GOQDs. The deduction is confirmed by the time-resolved fluorescence-delay curve (Fig. 5c). The PL lifetimes of PQDs aqueous solution are estimated to be 5.1 ns (2%) and 15.4 ns (98%), while those of GOQDs aqueous solution are 4.6 ns (18%)

and 12.4 ns (82%). It is supposed that the surface state with long PL lifetime and sp^2 domains with short PL lifetime serve as PL centers together. The emission of surface state is mainly determined by the type and quantity of surface functional groups, irrelevant with excitation wavelength. Meanwhile, the emission of sp^2domains is dependent on their sizes. Different sizes of sp^2 domains can be excited by different excitation wavelengths.[7] According to the measured PL lifetimes, we know that PL of PQDs mainly comes from the surface state, and that of GOQDs partly comes from sp^2 domains. As a result, PQDs exhibit apparent excitation-independent PL behavior, which is rather dissimilar to GOQDs and other carbon-based dots (Fig. S5).[5,11,14,32]

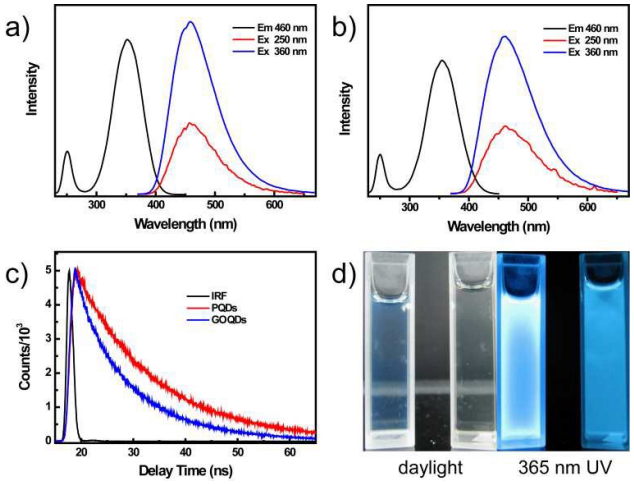

Fig. 5 PL spectra of (a) PQDs and (b) GOQDs aqueous solution (1 μg/ml). (c) Fluorescence life time decay profile of PQDs and GOQDs aqueous solution (1 μg/ml) under excitation at 405 nm. The emission was monitored at 460 nm. (d) Photographs of PQDs (left) and GOQDs (right) aqueous solution (10 μg/ml) under daylight and 365 nm UV. Note: PQDs exhibit obvious blue light under daylight excitation.

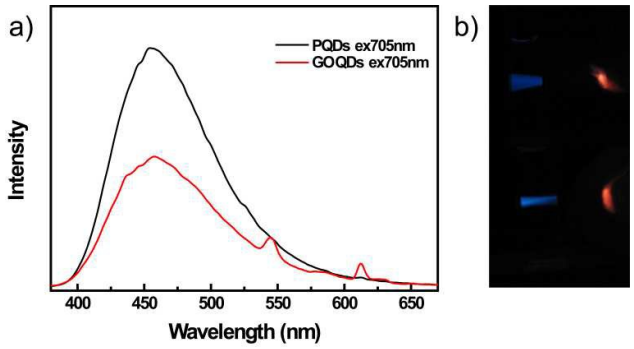

Fig. 6 (a) Two-photon-induced PL spectra of PQDs and GOQDs aqueous solution (10 μg/ml). (b) Photographs of PQDs (up) and GOQDs (down) aqueous solution (10 μg/ml) excited at 705 nm.

On the other hand, PQDs and GOQDs also exhibit obvious two-photon induced PL property (Fig. 6).They can be excited by long wavelength light (from 650 to 800 nm) with the up converted emissions in the range from 400 to 600 nm. The maximum emission peaks excited at 705 nm coincide with that excited at 360 nm, indicating that the same PL centers are responsible for the two-photon PL. The two small peaks at 545 and 612 nm in the two-photon PL spectra of GOQDs indirectly prove the above discussion. That is, there are more than one PL centers in GOQDs. The PQDs and GOQDs exhibit excellent stability at atmosphere condition, however, high-power UV radiation can partly quench the PL of PQDs and GOQDs (Fig. S6).

It has been known that N-doping can efficiently improve QY of carbon-based dots.[31,33,34] Here in this study, DETA exerts a great influence on QY of PQDs and GOQDs. The QY values of PQDs and GOQDs without DETA are only 12.3 and 4.2 %, respectively. Therefore, we claim that the amide groups play an important role in the PL property of PQDs and GOQDs.[35,36] C=O of amide can enhance the electron cloud density of PQDs and GOQDs through the conjugated effect with C=C. Additionally, –NH is a typical electron-withdrawing group, so that the amide groups can serve as not only electron acceptors but also electron donors, eventually leading to more efficient PL emission.[37]According to the results of element analysis (Table S1) and TGA (Fig. S7), the PQDs have lower C/N ratio and more weight loss at the decomposition temperature of amide group than GOQDs, which well illustrates the much higher QY of PQDs than that of GOQDs. To further prove our viewpoint, effect of pH value on PL property of PQDs and GOQDs was investigated (Fig. 7 and Fig. S8). It is seen that the PL intensities and lifetime of PQDs and GOQDs keep constant within the pH range 4-11, but drastically decrease at low or high pH. According to the time-resolved fluorescence-delay analysis of PQDs and GOQDs (Table S3 and S4), the decrease of PL lifetime mainly comes from the surface state. The percentage of the lifetime of PQDs from surface state decreases from 98% to 60% or 55% in strong acidic or strong base condition. This is because the amide groups are very unstable and would be easily hydrolyzed to carboxyl in strong acidic or strong base conditions, which leads to the evident decrease of the PL intensities of PQDs and GOQDs at low or high pH value.

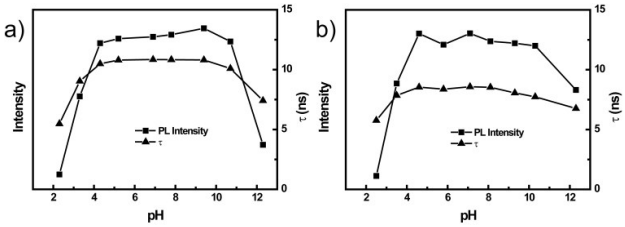

Fig. 7 Effect of pH value on PL intensity and lifetime of (a) PQDs and (b) GOQDs aqueous solution (10 μg/ml). 0.1 M NaOH and HCl were used to adjust the pH value.

Due to the high sensitivity and selectivity, GOQDs have been used as a fluorescent probe for the detection of metal ions.[4,32,33,38,39] However, the fluorescence quenching mechanism still remains elusive. Previous reports confirmed that electron transfer or aggregation induced by coordination between metal ions and carboxyl groups on the surface of GOQDs were the main reason for the fluorescence quenching.[4,32,33,38,39] However, in the present study, the electron transfer or coordination is only the necessary condition but not the sufficient condition.

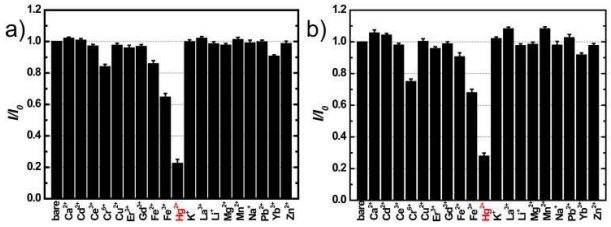

Fig. 8 Selectivity of (a) PQDs and (b) GOQDs to Hg^{2+} over other metal ions. PQDs and GOQDs: 1μg/ml; Na^+, K^+, Ca^{2+}, Mg^{2+}: 2 mM; other: 0.05 mM; I/I_0: PL intensity ratio of the QDs solution in the absence and presence of various metal ions.

To investigate the quenching mechanism of PL property, effect of various metal ions on the PL intensity of PQDs and GOQDs were studied. As shown in Fig. 8, only Hg^{2+} could effectively quench PL of PQDs and GOQDs, meanwhile, the counter ions of Hg^{2+} has little effect on the PL of PQDs and GOQDs (Fig S9), meaning that PQDs and GOQDs have high selectivity for Hg^{2+}. The marginal quenching effect produced by Fe^{3+} and Cr^{6+} is attributed to their strong absorption at the mentioned excitation wavelength (Fig. S10). According to the previous report,[39] the high selectivity for Hg^{2+} should originate from the coordination between Hg^{2+} and carboxylate or hydroxyl groups, which induces aggregation of PQDs or GOQDs and accelerates non-radiative recombination of excitons through an effective electron transfer process. However, other metal ions like Fe^{3+}, Cu^{2+}, Pb^{2+}, Cd^{2+}, La^{3+}, Fe^{2+} and Mn^{2+} also have rather high formation constants with carboxylate group (Table S5).[40] Especially, the formation constant of Fe^{3+} is higher than that of Hg^{2+}, but Fe^{3+} exhibits much less quenching effect on PQDs and GOQDs than Hg^{2+}. The result indicates that other unknown interaction must exist between Hg^{2+} and PQDs or GOQDs.

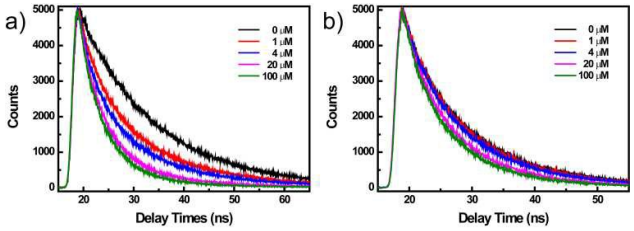

Fig. 9 Fluorescence lifetime decay profile of (a) PQDs and (b) GOQDs aqueous solution (1 μg/ml) with different Hg^{2+} concentrations under excitation at 405 nm. The emission was monitored at 460 nm.

To find out the intrinsic reason for the PL quenching mechanism, time-resolved fluorescence-delay curves of PQDs and GOQDs in the solution with different concentrations of Hg^{2+} were recorded (Fig. 9, Table S6 and S7). The average PL lifetime of PQDs decreases by 41.2 % when the concentration of Hg^{2+} increases from 0 to 100 μM. More importantly, the composition of the lifetime has been greatly changed with a rise in Hg^{2+} concentration. The percentage of lifetime resulting from surface state decreases from 98 % to 25 % when the concentration of Hg^{2+} increases from 0 to 100 μM, while the percentage of lifetime from sp^2 domains increases from 2 % to 75 %. It clearly shows that Hg^{2+} can only quench the PL from surface state and has little effect on the PL from sp^2 domains. The GOQDs have a similar trend with less change in the average PL lifetimes and the composition of lifetime, because more sp^2 domains take part in the PL lifetimes. The fluorescence emission of the PQDs or GOQDs from surface state is mainly attributed to the radiative recombination of the photo-induced electrons and holes on the surface of PQDs or GOQDs. In other words, the metal ions with strong electron accepting ability would prevent the radiative recombinations of the photo-induced electrons and holes and quench the fluorescence emission. The electrode potential of Hg^{2+} is 0.92 V, which is much higher than that of other metal ions like Fe^{3+} (0.771 V), Cu^{2+} (0.3419 V), Pb^{2+} (-1.262 V), Cd^{2+} (-0.403 V), La^{3+}(-2.522 V), Fe^{2+} (-0.477 V) and Mn^{2+} (-1.158 V) (Table S8),[40] implying that Hg^{2+} has more strong electron accepting ability than others. Therefore, only Hg^{2+} is allowed to efficiently quench the PL of PQDs and GOQDs.

It is worth noting that other oxidants with strong electron accepting ability such as H_2O_2, NaClO and $NaClO_3$ exhibit poorer quenching effect on the GOQDs as compared to Hg^{2+} (Fig. S11). It means that electron accepting strength is not the single factor for the quenching effect. To get more information about the PL quenching mechanism, the quenching effect of Hg^{2+} on the PL property of PQDs and GOQDs in the presence of other metal ions and EDTA was investigated (Fig. S12). It is seen that the metal ions except Fe^{3+} and Cr^{6+} have little quenching effect on the PQDs and GOQDs, but the quenching effect is greatly enhanced after the addition of Hg^{2+} except Fe^{3+}. Meanwhile, the quenching effect of only Hg^{2+} is more significant than that of Hg^{2+} coexisting with other metal ions. Furthermore, the quenched PQDs or GOQDs can be almost completely recovered when a certain amount of EDTA was added. EDTA is a strong chelator for metal ions, which could remove the metal ions including Hg^{2+} on the surface of PQDs or GOQDs. In this context, the coordination between Hg^{2+} and carboxylate or hydroxyl groups on the surface of PQDs or GOQDs is necessary for the quenching effect. Due to the higher formation constant of Fe^{3+} with carboxylate groups, Hg^{2+} has little quenching effect on PQDs or GOQDs in the presence of Fe^{3+}.

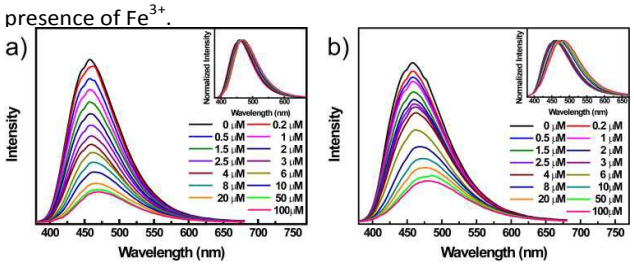

Fig. 10 PL spectra of (a) PQDs and (b) GOQDs aqueous solution (1 μg/ml) with different Hg^{2+} concentrations (excited at 360 nm). Insert: normalized emission spectra.

The sensitivity of PQDs and GOQDs to Hg^{2+} was assessed (Fig. 10). PL intensity of PQDs or GOQDs gradually decreases with increasing the concentration of Hg^{2+}. There is a linear relationship over the range from 0 to 10 μM (Fig. S13). However, the PL intensity of PQDs or GOQDs keeps nearly unchanged for the Hg^{2+} concentration from 20 to 100 μM, and the emission peak of PQDs or GOQDs has an obvious red shift in the case of high concentration Hg^{2+}. This phenomenon demonstrates that Hg^{2+} can only quench the PL from surface

state and has little effect on the PL from sp^2 domains. Moreover, the detection ranges of PQDs and GOQDs can be adjusted by changing the concentrations of PQDs and GOQDs (Fig. S14).

According to the discussion above, we can conclude that the mechanism involved in the PL quenching lies in the transition of the photo-induced electrons from the surface of PQDs or GOQDs to Hg^{2+}. The strong interaction, like coordination between Hg^{2+} and the functional groups on the surface of PQDs or GOQDs, is the precondition to realize the transition. Due to the high selectivity and sensitivity of PQDs and GOQDs to Hg^{2+}, the PQDs and GOQDs can be used as sensor for quantitative detection of Hg^{2+} in aqueous solution.

4 Conclusions

The N doped GOQDs and PQDs with one-photon-induced and two-photon-induced PL property were developed through rapid one-step microwave assisted pyrolysis of CA and DETA in different reaction solvents. DETA played an important role in the formation of GOQDs and PQDs. The PL of GOQDs and PQDs was proved to come from both surface state and sp^2 domains. The amide groups that serve as electron acceptors and electron donors contributed to the high QY of GOQDs and PQDs. The PL from surface state can be efficiently quenched through the transition of the photo-induced electrons from the surface of GOQDs and PQDs to Hg^{2+} induced by the coordination between Hg^{2+} and the functional groups on the surface of GOQDs and PQDs. Due to the high selectivity and sensitivity of GOQDs and PQDs to Hg^{2+}, the as-prepared GOQDs and PQDs can be used for quantitative detection of Hg^{2+} in aqueous solution

Acknowledgements

The authors are grateful for the support of the Science and Technology Program of Guangdong Province (Grant: 2010A011300004), the project of key technological breakthrough for emerging industries of strategic importance (Grants: 2011A091102001 and 2011A091102003), and Natural Science Foundation of China (Grant: U1201243 and 51503184).

Notes and references

1 S. Zhu, S. Tang, J. Zhang and B. Yang, *Chem.Commun.*,2012, **48**, 4527.
2 K. P. Loh, Q. L. Bao., G. K. Eda. and M. Chhowalla, *Nat. Chem.*,2010, **2**, 1015.
3 J. Shen, Y. Zhu, X. Yang and C. Li, *Chem.Commun.*,2012, **48**, 3686.
4 D. Wang, L. Wang, X. Dong, Z. Shi and J. Jin, *Carbon*,2012, **50**, 2147
5 Y. Li, Y. Hu, Y. Zhao, G. Shi, L. Deng, Y. Hou and L. Qu, *Adv.Mater.*,2011, **23**, 776.
6 J. H. Shen, C. Chen, X. L. Yang and C. Z. Li, *Chem.Commun.,* 2011, **47**, 2580.
7 M. Zhang, L. Bai, W. Shang, W. Xie, H. Ma, Y. Fu, D. Fang, H. Sun, L. Fan, M. Han, C. Liuand S. Yang, *J. Mater. Chem.*,2012, **22**, 7461.
8 F. Liu, M. H. Jang, H. D. Ha, J. H. Kim, Y. H. Cho and T. S. Seo, *Adv.Mater.*,2013, **25**, 3657.
9 X. T. Zheng, A. Than, A. Ananthanaraya, D. H. Kim and P. Chen, *ACSNANO*,2013, **7**, 6278.
10 J. Peng, W. Gao, B. K. Gupta, Z. Liu, R. Romero-Aburto, L. Ge, L. Song, L. B. Alemany, X. Zhan, G. Gao, S. A. Vithayathil, B. A. Kaipparettu, A. A. Marti, T. Hayashi, J. J. Zhu and P. M. Ajayan, *Nano. Lett.*,2012, **12**, 844.
11 D. Pan, J. Zhang, Z. Li and M. Wu, *Adv.Mater.*,2010, **22**, 734.
12 J. Lu, J. X. Yang, J. Z. Wang, A. Lim, S. Wang and K. P. Loh, *ACSNANO*,2009, **3**, 2367.
13 S. Zhu, J. Zhang, C. Qiao, S. Tang, Y. Li, W. Yuan, B. Li, L. Tian, F. Liu, R. Hu, H. Gao, H. Wei, H. Zhang, H. Sun and B. Yang, *Chem. Commun.*,2011, **47**, 6858.
14 S. Zhu, J. Zhang, S. Tang, C. Qiao, L. Wang, H. Wang, X. Liu, B. Li, Y. Li, W. Yu, X. Wang, H. Sun and B. Yang, *Adv. Funct. Mater.*,2012, **22**, 4732.
15 Y. Dong, J. Shao, C. Chen, H. Li, R. Wang, Y. Chi, X. Lin and G. Chen, *Carbon*,2012, **50**, 4738.
16 L. Li, G. Wu, G. Yang, J. Peng, J. Zhao and J. J. Zhu, *Nanoscale*,2013, **5**, 4015.
17 I. P. Hamilton, B. Li, X. Yan and L. S. Li, *Nano. Lett.*,2011, **11**, 1524.
18 R. Liu, D. Wu, X. Feng and K. Mullen, *J. Am. Chem. Soc.*,2011, **133**, 15221.
19 X. Yan, Q. Li and L. S. Li, *J. Am. Chem. Soc.*,2012, **134**, 16095.
20 J. Ju and W. Chen, *Biosens. Bioelectron.*, 2014, **58**, 219.
21 J. Jiang, Y. He, S. Li and H. Cui, *Chem. Commun.*,2012, **48**, 9634.
22 S. Qu, X. Wang, Q. Lu, X. Liu and L. Wang, *Angew.Chem. Int. Ed.*,2012, **51**, 12215.
23 P. Zhang, W. Li, X. Zhai, C. Liu, L. Dai and W. Liu, *Chem. Commun.*,2012, **48**, 10431.
24 X. Zhai, P. Zhang, C. Liu, T. Bai, W. Li, L. Dai and W. Liu, *Chem. Commun.*,2012, **48**, 7955.
25 L. Tang, R. Ji, X. Cao, J. Lin, H. Jiang, X. Li, K. S. Teng, C. M. Luk, S. Zeng, J. Hao and S. P. Lau, *ACSNANO*,2012, **6**, 5102.
26 S. Chen, X. Hai, C. Xia, X. W. Chen and J. H. Wang, *Chem. Eur. J.*,2013, **19**, 15918.
27 S. Zhu, Q. Meng, L. Wang, J. Zhang, Y. Song, H. Jin, K. Zhang, H. Sun, H. Wang and B. Yang, *Angew. Chem. Int. Ed.*,2013, **52**, 3953.
28 Z. Qian, J. Ma, X. Shan, H. Feng, L. Shao and J. Chen, *Chem. Eur. J.*, 2014, **20**, 2254.
29 X. F. Jia, J. Li and E. K. Wang, *Nanoscale*,2012, **4**, 5572.
30 X. Wu, F. Tian, W. Wang, J. Chen, M. Wu and J. X. Zhao, *J. Mater. Chem C.*,2013, **1**, 4676.
31 J. J. Huang, Z. F. Zhong, M. Z. Rong, X. Zhou, X. D. Chen and M. Q. Zhang, *Carbon*, 2014, **70**, 190.
32 L.L. Li, J. Ji, R. Fei, C.Z. Wang, Q. Lu, J.R. Zhang, L.P. Jiang and J.J. Zhu, *Adv. Funct. Mater.*,2012, **22**, 2971.
33 H. Sun, N. Gao, L. Wu, J. Ren, W. Wei and X. Qu, *Chem. Eur. J.*,2013, **19**, 13362.
34 J. Ju and W. Chen, *Anal. Chem.*, 2015, **87**, 1903.
35 M. J. Krysmann, A. Kelarakis, P. Dallas and E. P. Giannelis, *J. Am. Chem. Soc.*,2012, **134**, 747.
36 H. Tetsuka, R. Asahi, A. Nagoya, K. Okamoto, I. Tajima, R. Ohta and A. Okamoto, *Adv. Mater.*,2012, **24**, 5333.
37 S. H. Jin, D. H. Kim, G. H. Jun, S. H. Hong and S. Jeon, *ACS NANO*,2013, **7**,1239.
38 Y. X. Qi, M. Zhang, Q. Q. Fu, R. Liu and G. Y. Shi, *Chem. Commun.*,2013, **49**, 10599.
39 Y. Guo, Z. Wang, H. Shao and X. Jiang, *Carbon*,2013, **52**, 583.
40 J. G. Speight, *LANGE'S HANDBOOK OF CHEMISTRY*, McGRAW-HILL, New York, 16rd edn, 2005.